A TEST VALIDATED MODEL OF PLATES WITH CONSTRAINED VISCOELASTIC MATERIALS

Anne-Sophie Plouin and **Etienne Balmès**

École Centrale Paris
MSSMat
92295 Châtenay-Malabry, France

Abstract

Surface damping treatments by viscoelastic materials are often considered nowadays to enhance dissipation in sheet metal and laminated glass parts. Constraining layers are needed to increase shear levels in the viscoelastic which is the primary source of dissipation. The damping behavior of such sandwich types structures is strongly influenced by the characteristics of the constraining layer and the deformation modes of the structure. It is first shown that finite element models based on classical laminated plate theory (CLPT) do not allow a proper representation of boundary conditions of the viscoelastic and the constraining layer which leads to an inaccurate prediction of the behavior of the damped structure. A layered shell/solid/shell model is introduced and shown to correct these shortcomings. The validity of the proposed model is demonstrated by correlation with experimental results obtained on the GARTEUR SM-AG-19 testbed. The damping treatment of this structure is a layer of ISD112 (a viscoelastic manufactured by 3M) constrained by an aluminum plate. Test and analysis damping levels are first shown to be very well correlated. Temperature dependence and computational times are finally discussed to give further insight in the proposed methodology.

1 INTRODUCTION

Surface damping treatments with viscoelastic materials are often introduced in existing structure to alleviate noise and vibration problems. Free-layer treatments lead to traction-compression deformations of the viscoelastic, which needs to be stiff in order to carry a significant fraction of the load and thus dissipate a noticeable fraction of the energy. Constrained layer treatments use the stiffness of the constraining layer to induce high levels of shear deformation in the viscoelastic and are thus typically more efficient.

Constraining layer effects can be easily introduced in sheet metal and laminated glass parts and have led to the development of commercial products such as *Solconfort* by SOLLAC which seek to use the enhanced damping in noise and vibration reduction applications. The development of models allowing the design of the dynamic behavior of such structures is the ultimate aim of the work presented here.

The dynamics of sandwich type structures with viscoelastic materials, depends not only on the characteristics of the viscoelastic (frequency, temperature and geometry) but also very significantly on the geometry and boundary conditions of the constraining layer. The Classical Laminated Plate Theory (CLPT) leads to a finite element model which does not represent shear deformations in the viscoelastic very well and cannot take in account the boundary conditions of the damping and constraining layers. A shell/solid/shell model is thus introduced in this paper. The resulting model uses about twice as many degrees of freedom but the use of model reduction techniques for viscoelastic structures [1] lead to fairly reasonable computational costs. Section 2 discusses theoretical aspects of the CLPT, the new three layer model, and model reduction techniques used for actual computations.

These theoretical results are then applied to the GARTEUR SM-AG-19 testbed [2] in section 3. This structure designed for ground vibration testing was tested by 12 European laboratories to evaluate the reliability of various modal testing as a Round Robin exercise. Unlike previous exercises Round Robin exercises in modal testing [3], significant damping levels were obtained through the use of a constrained viscoelastic layer.

Predictions of modal characteristics are first made for a wing only model in order to compare the CLPT elements and the three layer model. The accuracy of the three layer model is then demonstrated by correlating experimental results of the GARTEUR exercise with predictions for the entire structure. Temperature dependence and computational times are finally discussed to give further insight in the proposed methodology.

2 MODELING OF VISCOELASTIC SANDWICH PLATES

2.1 Classical Laminated Plate Theory

The Classical Laminated Plate Theory (CLPT) models plates constituted by two or more laminae. The kinematics of each ply are assumed to follow the Reissner-Mindlin thick plate assumptions leading to a linear variation of the strain field through the thickness

$$\{\epsilon\} = \left\{e^0\right\} + z\{\kappa\} \quad \{\gamma\} = \left\{\gamma^0\right\} \tag{1}$$

where $\{\epsilon\}$ is associated to the membrane and bending deformation and $\{\gamma\}$ to the shear deformation.

The constitutive relations for each layer are

$$\{\sigma_j\} = [Q_{ij}]\{\epsilon_j\} \quad \{\tau_i\} = [C_{ij}]\{\gamma_j\} \tag{2}$$

where Q_{ij} $(i,j = 1,2,6)$ are the reduced stiffness for plane stress and C_{ij} $(i,j = 4,5)$, the ply shear stiffness.

The constitutive relations for the plate are deduced from integration of (2) and use of (1)

$$\left\{ \begin{array}{c} N_i \\ M_i \end{array} \right\} = \left[\begin{array}{cc} A_{ij} & B_{ij} \\ B_{ij} & D_{ij} \end{array} \right] \left\{ \begin{array}{c} e_j^0 \\ \kappa_j \end{array} \right\} \quad \{i,j = 1,2,6\} \tag{3}$$

with $\{A_{ij}, B_{ij}, D_{ij}\} = \int_{-h/2}^{h/2} Q_{ij}\{1, z, z^2\} dz \quad \{i,j = 1,2,6\}$ where the membrane force and bending moment resultants are defined as usual.

The form of the displacement field leads to constant transverse shear stresses through the thickness of the plate, which are incompatible with free boundary conditions on the upper and lower faces and the global equilibrium of the plate. To solve this problem linked to the use of a first order theory, shear correction factors are usually introduced in the transverse shear constitutive relations: γ_{xz}^0 and γ_{yz}^0 are respectively replaced by $k_1\gamma_{xz}^0$ and $k_2\gamma_{yz}^0$. The shear constitutive relations for the plate are thus given by

$$\left\{ \begin{array}{c} T_y \\ T_x \end{array} \right\} = \left[\begin{array}{cc} k_2^2 A_{44} & k_1 k_2 A_{45} \\ k_1 k_2 A_{45} & k_1^2 A_{55} \end{array} \right] \left\{ \begin{array}{c} \gamma_{yz}^0 \\ \gamma_{xz}^0 \end{array} \right\} \tag{4}$$

with $A_{ij} = \int_{-h/2}^{h/2} C_{ij} dz \quad \{i,j = 4,5\}$ which can be written $\{T\} = \left[\tilde{A}\right]\left\{\gamma^0\right\}$

The approach used here to determine k_1 and k_2 is based on Chow [4] who starts from the assumption of cylindrical bending of the x and y axes to determine the shear factors. Taking the case of cylindrical bending along the x axis, the constitutive relations for each ply take the form

$$\sigma_i^k = Q_{ij}^k (B_{jm}^* + z D_{jm}^*) M_m \quad \{i,j,m = 1,6\} \tag{5}$$

where $\sigma_1 = \sigma_x$ and $\sigma_6 = \sigma_{xy}$. B^* and D^* are defined by inverting (3)

$$\left\{ \begin{array}{c} e_i^0 \\ \kappa_i \end{array} \right\} = \left[\begin{array}{cc} A_{ij}^* & B_{ij}^* \\ B_{ij}^* & D_{ij}^* \end{array} \right] \left\{ \begin{array}{c} N_j \\ M_j \end{array} \right\} \quad \{i,j = 1,6\} \tag{6}$$

Combining equation (5) with the equilibrium equations and the global equilibrium of the plate yield the following form of the shear transverse stress

$$\tau_i^k = c_i^k - Q_{ij}^k \frac{z}{2} (2B_{jm}^* + z D_{jm}^*) T_m \quad \{i,j,m = 1,6\} \tag{7}$$

where $T_1 = T_x$ and $T_6 = T_y$. The constant c_i^k is determined by the boundary conditions, assuming that τ_{xz} vanishes on the bottom ply. The value of k_1 is obtained by equalizing the coefficient of T_x in the shear strain energies deduced from (4) and (7) which are defined respectively by

$$\{T\}^T \left[\tilde{A}\right]^{-1} \{T\} \quad \text{and} \quad \int \left\{\tau^k\right\}^T \left[S^k\right] \left\{\tau^k\right\} dz \tag{8}$$

where $[S_{ij}]$ $(i,j = 4,5)$ is the transverse shear compliance matrix.

For orthotropic plies, the shear correction factor is given by

$$k_1^2 = \frac{1}{A_{55}} \left[\int_{-h/2}^{h/2} S_{55} \left(h^k(z)\right)^2 \right]^{-1} \tag{9}$$

where $h^k(z) = c_1^k + \frac{Q_{11} z}{2(A_{11} D_{11} - B_{11}^2)} (2B_{11} - A_{11} z)$

The viscoelastic materials considered in this paper are supposed to be described by a complex frequency dependent modulus E_v as usual in linear viscoelasticity [5, 6]. The computation of the shear correction factor is thus not trivial. The assumption made here is to take constant shear correction factors corresponding to the static problem at $\omega = 0$, the viscoelastic modulus is then real.

Extensions that were not considered, but probably would not correct the major shortcomings of the CLPT model, would be to recompute the correction factor using the storage modulus of the viscoelastic at each frequency and to introduce a correction for the imaginary part of the stiffness matrix using a constant loss factor for the elastic materials.

2.2 The 3L*ayer* shell/solid/shell model

As will be shown in section 3.2, the CLPT model has significant shortcomings. To alleviate these problems, this study introduces an alternative finite element model for sandwich plates. The specificity of this model is to use classical finite elements for each layer of the sandwich. The constrained and constraing metal layers use two 4-node/24-DOF classical shell elements and the viscoelastic layer uses a 8-node/24-DOF solid element (See Figure 1). For the metallic layers modeled with shells, the element nodes are off-set to the plane in contact with the viscoelastic instead of the standard midplane. This results in coincident nodes and thus an acceptable coupling. Shell rotations are not coupled even though it is understood that this results in a non-conforming finite element formulation. For this study, the quad4

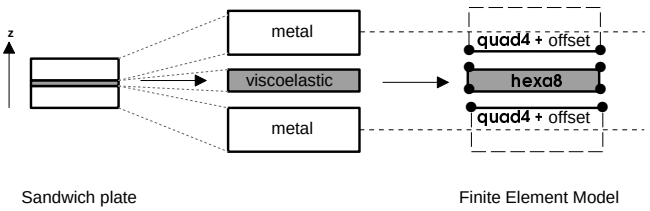

Figure 1: The 3L shell/solid/shell element construction

thick shell element of the SDT [7] is used. This element uses a `Q4WT` formulation for the membrane and a `Q4Gamma` formulation for bending, with the classical 5/6 shear correction factor. The 3L model thus leads to a 4-node/48-DOF element defined in the upper or lower plane of the viscoelastic layer. This element comprises twice the number of DOFs compared to a classical thick shell element but the addition of DOFs is compensated by reduction techniques described in the next subsection.

2.3 Reduction of viscoelastic models

This section summarizes model reduction techniques introduced in [1] to obtain reasonable computational costs and used in this study. For the examples considered here, one will only consider a single type of viscoelastic material while the rest of the structure is assumed to be elastic. The form of the input/output model is thus

$$\begin{array}{c}\left[-M\omega^2 + K_e + E_v(\omega)K_v\right]\{q(\omega)\} = [b]\{u(\omega)\} \\ \{y(\omega)\} = [c]\{q(\omega)\}\end{array} \tag{10}$$

where K_e is the elastic part of the stiffness matrix and K_v the viscoelastic part for a unit Young's modulus E_v.

The traditional approach for computing frequency responses is to project the model (10) on a basis $[T]$, with the assumption that $\{q\} \simeq [T]\{q_R\}$. The projection of model on the considered basis leads to a low order model (as many generalized DOFs as independent columns in the matrix T)

$$\begin{array}{c}\left[-T^T M T\omega^2 + T^T K(\omega) T\right]\{q_R(\omega)\} = \left[T^T b\right]\{u(\omega)\} \\ \{y(\omega)\} = [c]\{q_R(\omega)\}\end{array} \tag{11}$$

For a model with a real and frequency independent stiffness matrix, the model is traditionally projected on a basis containing the first NR normal modes $\phi_{j=1,NR}$ covering the frequency range of interest and the static response to the considered load $\left[K^{-1}[b]\right]$.

The projection can be applied to a frequency dependent damped model by replacing the normal modes by either normal modes computed for the value of the real part of the stiffness at one or two frequencies [8] or pseudo-normal modes [1] $\tilde{\phi}_{j=1,NR}$ which are defined as the solutions of the generalized eigenvalue problem

$$\left[-M\tilde{\omega}_j^2 + \mathrm{Re}(K(\tilde{\omega}_j))\right]\tilde{\phi}_j = 0 \tag{12}$$

To these modes which characterize the low frequency response, one adds the static response to unit load(s) $[b]$ [8] to account for low frequency effects of high frequency modes. The projection basis thus has the form

$$[T_A] = \left[\begin{array}{cc}\tilde{\phi}_{j=1,NR} & [\mathrm{Re}\{K(\omega_{\max})\}]^{-1}[b]\end{array}\right]. \tag{13}$$

As shown in [1], better accuracy on the damping predictions is obtained by introducing a first order correction to the basis $[T_A]$ by computing the static response to the load generated by the imaginary part of the stiffness when exciting a given normal or pseudo-normal mode

$$[T_{Cj}] = [\mathrm{Re}\{K(\tilde{\omega}_j)\}]^{-1}[\mathrm{Im}\{K(\tilde{\omega}_j)\}]\left\{\tilde{\phi}_j\right\}. \tag{14}$$

The basis $[T_A \quad T_{Cj=1,NR}]$ contains twice the number of normal modes in the considered band but the accuracy improvement and increased confidence in the results typically justify the relatively minor increase of computational cost.

3 ILLUSTRATIONS

3.1 Model of the GARTEUR testbed

The GARTEUR SM-AG-19 structure [2] was tested by 12 laboratories from European companies, research centers and universities in France, Germany, the Netherlands, Sweden and the United Kingdom as a Round Robin exercise to evaluate the reliability of various modal testing. The details of the final design are summarized in [2]. The major difficulty of the test was a group of three very close modes. Most of the participants being involved in ground vibration testing of aircraft, the testbed was made heavy (50 kg) to try minimizing measurement equipment loading even when using equipment designed to test much larger structures. The availability of many openly available test results on this structure motivated its use in the present study even though short term applications are really the prediction of damping levels in objects made with steel/visco/steel sandwiches such as *Solconfort* made by SOLLAC.

The finite element model used in this study is shown in Figure 2. The global model uses 2262 DOFs, 262 nodes, 228 elements including 1380 DOFs, 115 nodes, 180 elements for the wing.

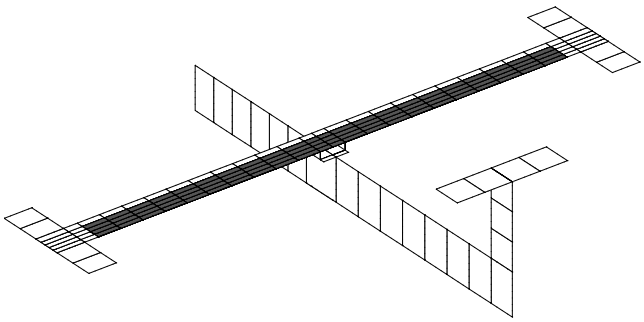

Figure 2: Finite element model of the testbed

The undamped part of the structure is modeled with 4-node/24-DOF plate elements. The damped part of the wing is modeled using a 12 by 4 grid of CLPT shells or 3L models (see section 2). The elastic properties taken for the aluminium parts are $E = 72\ 10^9 N/m^2$, $\nu = 0.3$ and $\rho = 2.7\ 10^3 kg/m^3$. Real, temperature and frequency independant values used for the viscoelastic are $\nu = 0.45$ and $\rho = 1.2 kg/m^3$.

The damping treatment is composed of a $1.7m \times 76mm \times 0.05mm$ viscoelastic self-adhesive film constrained by a $1mm$ thick aluminium plate and set on the wing which is a rectangular $2m \times 100mm \times 10mm$ aluminium plate. Two $100mm \times 400mm \times 10mm$ rectangular drums are centered on each wing tip. The viscoelastic is the 3M-ISD112 acrylic polymer whose damping properties are provided by 3M [9] in the standard reduced temperature format. Considering the relation between frequency and temperature, the storage modulus and the loss factor are thus given as a function of $\omega\alpha_T$, where α_T, the temperature shift factor, is an absolute function of temperature [10].

$$E(\omega, T) = f(\omega\alpha_T(T)) \tag{15}$$

where $\text{Log}(\alpha_T) = -c_1(T - T_0)/(T - T_\infty)$.

The two first subplots of figure 3 give the master curves at $20°C$ of the 3M-ISD112 strorage modulus and loss factor. The properties for a specific temperature T are deduced from this curve by an off-set on the log-frequency axis of value $\text{Log}(\alpha_T(T)/\alpha_T(20))$, whose curve is given in the third subplot of figure 3.

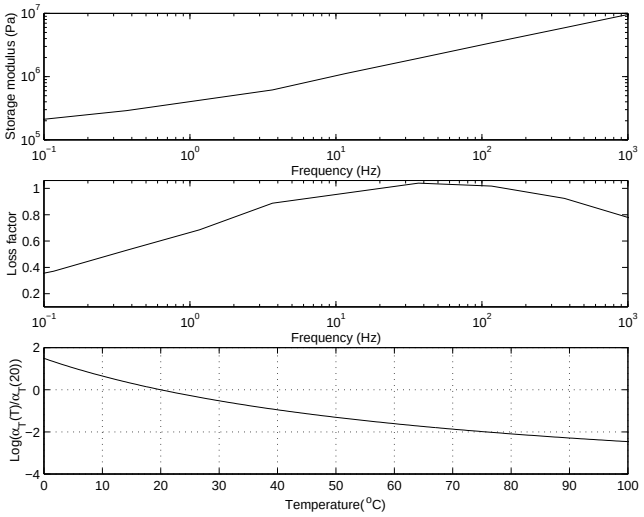

Figure 3: 3M-ISD112 master curve at $20°C$ and temperature shift factor

The GARTEUR testbed was designed to have relevant test modes in the 5 to 50 Hz range. Figure 3 indicates that the room-temperature loss factor of the ISD112 is above 0.9 in this range which motivated the selection of this particular viscoelastic.

In the rest of the paper, an estimation of the damping ratio ζ linked to an approximation of the structural loss factor η will be used, considering the relationship $\eta \simeq 2\zeta$. The structural loss factor is predicted using the strain energy method adapted to composite structures. The principle of this method is that the structural loss factor can be estimated by the ratio of the dissipation energy to the strain energy in the undamped structure. For composite structures, the structural loss factor can thus be considered as the sum of the material loss factors weighted by the ratio of the elastic strain energy in the each part of the structure to the total strain energy in the undamped structure

$$\eta \simeq \frac{U_D}{U_S} = \frac{\sum_{(m)} \eta^{(m)} U_S^{(m)}}{\sum_{(m)} U_S^{(m)}} \tag{16}$$

where $\eta^{(m)}$ is the loss factor for each material, and U_D the dissipation energy of the entire structure. U_S represents the elastic stain energy of the entire structure and is equal to the sum of all $U_S^{(m)}$, the elastic strain energy of each part structure.

In practice, the modal damping ratio ζ is computed with the pseudo-normal modes using

$$\zeta(\tilde{\omega}_j) = \frac{1}{2} \frac{\left\{\tilde{\phi}_j\right\}^T [\eta_e K_e + \text{Im}(E(\tilde{\omega}_j))K_v] \left\{\tilde{\phi}_j\right\}}{\left\{\tilde{\phi}_j\right\}^T [\text{Re}(K(\tilde{\omega}_j))] \left\{\tilde{\phi}_j\right\}} \tag{17}$$

Test		FEM			MAC
ω (Hz)	ζ (%)	ω (Hz)	ζ (%)		
			$\eta_e = 0$	$\eta_e = 0.2\%$	
6.38	1.30	6.56	0.89	0.99	100
16.10	1.30	14.76	1.70	1.80	93
33.12	0.83	36.10	1.13	1.23	79
33.53	1.00	36.23	1.13	1.23	86
35.65	1.10	39.72	0.75	0.85	96
48.38	2.30	51.39	2.16	2.25	99
49.43	0.46	53.07	0.23	0.33	97
55.08	0.20	57.06	0.03	0.13	100

Table 1: MAC comparison on 24 sensors between experimental (GARTEUR participant C) and FEM modes

Table 1 gives the MAC comparison between experimental and computed pseudo-normal modes of the structure. The poor correlation for modes 3 and 4 is linked to the dissymmetry of the actual structure which leads to torsion modes that are not truly symmetric. This also affects mode 4 which is very close in frequency. For the present paper, which focuses on damping predictions, no further effort was done to determine the origin of the noticeable error on the second mode or to update the model to obtain better correlation of the frequencies.

3.2 Comparison between the CLPT elements and the 3L model

The purpose of this section is to show the respective ranges of applicability of the CLPT and 3L models. To do so, one will consider only the wing of the GARTEUR structure and use the fact that cuts in constraining layers are expected to have significant impact on the damping levels of various modes [11].

To motivate the use the 3L model, one first predicts the damping ratios of the two first modes of real the wing. Wing only tests were performed before assembly of the final structure and the

drums were then 10 cm longer. Table 2 shows the experimental and numerical damping ratios. The results obtained with the 3L model are slightly lower than those obtained for the wing with the damping treatment. The computations were performed assuming no damping in the aluminium parts. But tests carried out on the wing before addition of the damping treatment indicate some levels of dissipation. Taking into account a small loss factor for the aluminium would thus lead to better predictions of the 3L model. On the other hand, the CLPT element totally underpredicts both of the damping ratios. Even readjusting the loss factor of aluminium would not lead to a correct prediction.

mode	tests before treatment	tests after treatment	3L	CLPT
bending	0.3	1.1	0.9	1e-5
torsion	0.1	0.9	0.8	1e-6

Table 2: Damping ratios (%) for the GARTEUR wing only, estimated by the energy method

The results of the 3L model on the wing with the complete damping treatment (**case A**) encourage us to use it to examine the effects of cuts in the damping treatment. Two cases of cuts (see Figure 4) are considered here. In the first case (**case B**), one cut of 0.1 mm is done along the width of the damping treatment in the middle of the length while the second case (**case C**) contains a second 0.1 mm cut in length of the damping treatment. The models associated to the three cases have the same number of DOFs as the considered cuts are only one element wide and the model used for case A already uses the very narrow constraining layer elements that are removed for case B and C.

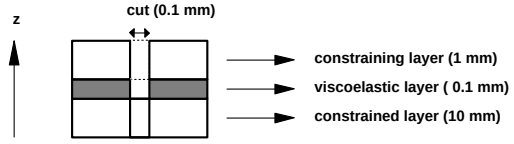

Figure 4: Detail of a cut in the damping treatment

To illustrate the validity of the CLPT and 3L models, one will assume elastic properties for the viscoelatic layer and analyze predicted modal frequencies and strain energy repartition (fraction of strain energy in the viscoelastic layer) for a modulus varying between the low frequency storage modulus of ISD112 ($\simeq 10^5 N/m^2$) to the modulus of aluminium $E_{alu} = 72\ 10^9 N/m^2$. The predicted frequencies are clearly expected to fall within the two limiting cases of the structure with no treatment ($10mm$ aluminium plate) and the structure where the viscoelastic is really aluminum ($11.1mm$ aluminium plate). These expected limits are plotted in figures 5 and 6 as dashdotted and dotted lines.

The variations for the first bending mode, shown in figure 5, are only given for cases A and B, case C yielding to the same results as case B. Similarly, the variations for the first torsion mode (figure 6) are only given for cases A and C as the results for case B are the same as case A. These results show that a cut in the length of the damping area has no effect on the modal characteristics for the bending mode whereas a cut in the width has no effect on the torsion mode.

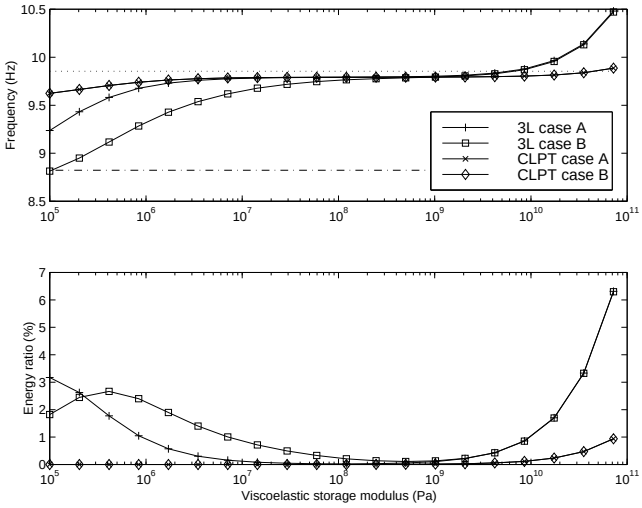

Figure 5: Frequencies and damping energy ratios of the first bending mode

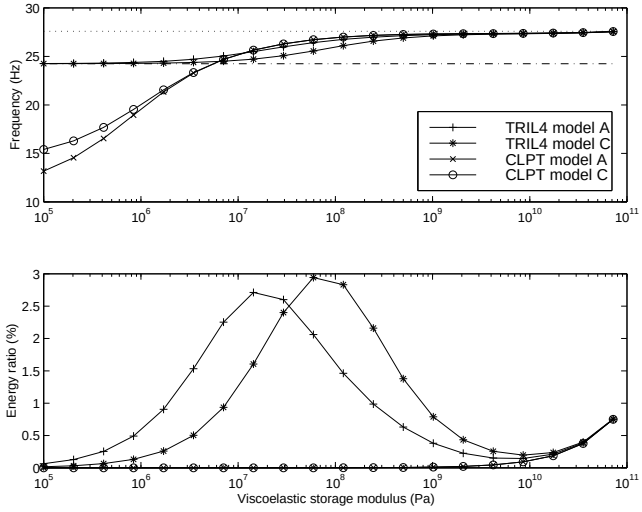

Figure 6: Frequencies and damping energy ratios of the first torsion mode

To analyse the performance of the CLPT model, one first notices that in case A for low moduli, the bending frequency does not tend to the lower frequency limit. This over-stiffening is due to the assumption of linear variation of strain through the thickness that is not verified and cannot be corrected by the shear correction factor. For the torsion mode, the frequencies obtained for low moduli are completely below the lower limit because the shear correction factor tends to zero. The determination of the correction factor based on cylindrical bending

solutions is not adapted for torsion. For high moduli, the response is as expected very accurate.

For both modes, the energy fractions in the viscoelastic (and thus the resulting damping predictions) are underpredicted for all but very high moduli. Moreover, only minor differences are visible between the modal characteristics of the three cases A, B and C with the CLPT element which indicates that it does not properly take cuts into account.

The validity of the CLPT model is thus poor at best for the cases of interest where the modulus of the viscoelastic is much lower than that of the constraining layers.

For high moduli ($\mathrm{Re}(E_v) \rightarrow E_{alu}$), the 3L model also overestimates the bending frequencies (torsion frequencies are correct for the whole range). This over-stiffening corresponds to a well known "locking" phenomenon typically illustrated by the inability of bilinear membrane elements to represent in-plane bending motion for high aspect ratio. The cases of interest here correspond to the low moduli range, where the element really works in shear and does so correctly. In the plots, one effectively sees modal frequencies converging with the lower frequency limit.

The energy ratio curves based on the 3L model show a peak indicating an optimum value of the viscoelastic modulus for which maximum damping is obtained. For the bending mode, the maximum damping ratio is 3.1% in case A and decrease at 2.7% in cases B and C whereas, for the torsion mode, the maximum damping ratio is 2.7% in case A and B and increase at 2.9% in case C. However, when a cut has an influence on the damping ratio of a given mode, one notes that the peak is obtained for a higher modulus than in case without cut. Depending on the actual variation of a viscoelastic modulus, cutting the damping treatment could then be a solution to get higher damping levels for specific modes.

3.3 Damping predictions for the entire structure

The 3L model will now be used to perform predictions of damping levels of the whole GARTEUR structure described in section 3.1. Only nine participants of the GARTEUR SM-AG-19 provided results complying with the test specification. The minimum, maximum and mean damping ratio values derived from these tests are given as the solid line envelope in figure 7. Computations based on the 3L model using damping estimator (17), and loss factors in the aluminum varying between 0 and 0.5% are then superposed. The match is extremely good except for mode 2 which is also poorly correlated in terms of mode shape (this poor correlation probably comes from the wing/fuselage link).

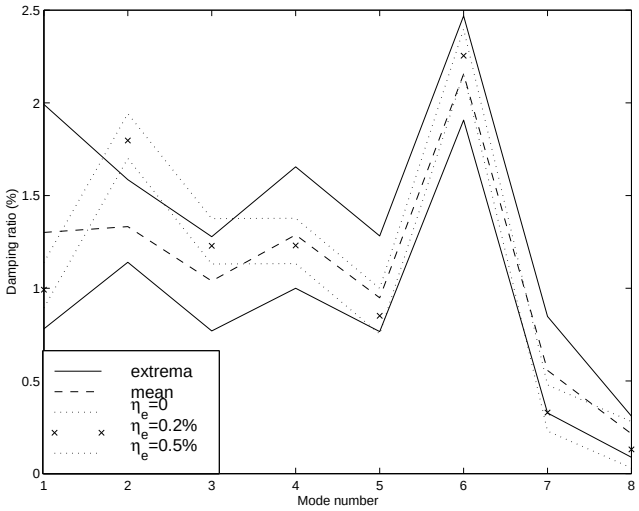

Figure 7: Comparison of the damping ratios between results of the GARTEUR round robin exercise [2] and computations based on the 3L model with various loss factors η_e in the elastic part of the structure

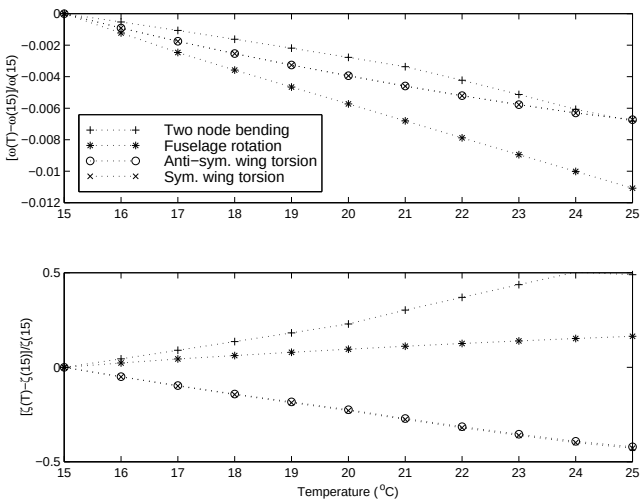

Figure 8: Influence of the temperature on the frequencies and damping ratios

For the previous computations, the temperature was assumed to be constant at $18°C$. However, the influence of the temperature can be significant on the damping level. Figure 8 shows the variations of the damping levels of the first four modes of the structure between $15°C$ and $25°C$. The frequencies of the four modes exhibit all a slight fall on the temperature range of interest (maximum fall of 0.01% for the fuselage rotation). For further predictions, the frequency can thus be estimated a priori on a temperature range with a unique computation at a mean temperature. For the two-node bending and fuselage rotation

modes of wing, the damping levels increase on the temperature range, specially the two node bending mode with a rise of 50%. On the other hand, for the two modes of wing torsion, the damping levels drops by 50% between $15°C$ and $25°C$.

task	CPU time (s)
assembly	25
20 normal modes	6
20 pseudo-modes	89
correction basis	7
full FRF/frq point	28
reduced FRF/frq point	5.9e-3
reduced corrected FRF/frq point	9.8e-3

Table 3: CPU times FRF predictions using SDT 3.1 [7] on a SGI R10000 processor

Model reduction is an important aspect of the proposed methodology. Computational times shown in table 3 indicate that the reduction phase takes about 2 or 3 times longer than model assembly. While this could be significantly improved, it would never go much below assembly times. The resolution of the full order viscoelastic problem is about 3000 times slower than the associated reduced version. This ratio is in part due to the use of the basic MATLAB sparse functions for the full order computation. But orders of magnitude in difference would still remain after optimization. Finally, it should be noted that reduction can be performed at a single temperature for studies of temperature dependence, thus giving another critical advantage in design studies.

4 CONCLUSION

A three layer shell/solid/shell model was demonstrated to be effective in modeling metal/visco/metal sandwich plates. The demonstration was based on comparisons with test results on the wing-only and full structure configurations of the GARTEUR SM-AG-19 testbed. For the full structure the variations between realistic damped models of the structure are lower than those found between various test results.

The 3 layer model is built using classical finite elements available in most commercial software. It was shown to be efficient at capturing the effect of cuts in the damping treatment leading to variations in the damping of various modes. Comparisons with results obtained with Classical Laminated Plate Theory showed the failure of this approach but also illustrated over-stiffening effects of the 3 layer model in cases with very stiff viscoelastics (which are not the focus of the present study).

The whole study was made possible by the use of model reduction techniques introduced in Ref. [1]. These techniques limit the impact of the increased number of degrees of freedom (the 3L model uses 2 layers of standard shell elements) and elements (three elements trough the thickness). Studies for more intricate models with tens of thousands DOFs are thus quite reasonable.

Further directions of research are the validation of the 3L model for sandwich shells and realistic industrial objects, use of identification techniques rather than energy ratio considerations to estimate loss factors, and introduction of a methodology to build dynamically equivalent time domain models.

References

[1] **Plouin**, **A**. and **Balmès**, **E**., *Pseudo-Modal Representations of Large Models with Viscoelastic Behavior*, IMAC, pp. 1440–1446, 1998.

[2] **Balmès**, **E**., *GARTEUR group on Ground Vibration Testing. Results from the test of a single structure by 12 laboratories in Europe*., IMAC, 1997, 1997.

[3] **Ewins**, **D**. and **Griffin**, **J**., *A State of the Art Assessment of Mobility Measurement Techniques - Results for the Mid-Range Structures (30-3000 Hz)*, Journal of Sound and Vibration, Vol. 78, No. 2, pp. 197–222, 1981.

[4] **Chow**, **T**., *On the Propagation of Flexural Waves in an Orthotropic Laminated Plate and its Response to an Impulsive Load*, J. Composite Materials, Vol. 5, pp. 306, 1971.

[5] **Bert**, **C**., *Material Damping: An Introductory Review of Mathematical Models, Measures, and Experimental Techniques*, Journal of Sound and Vibration, Vol. 29, No. 2, pp. 129–153, 1973.

[6] **Salençon**, **J**., Viscoélasticité, Presse des Ponts et Chaussés, Paris, 1983.

[7] **Balmès**, **E**., Structural Dynamics Toolbox 3.1 (for use with MATLAB), Scientific Software Group, Sèvres (France), info@sdtools.com, 1998.

[8] **Balmès**, **E**., *Model Reduction for Systems with Frequency Dependent Damping Properties*, IMAC, 1997.

[9] **3M**, *Scotchdamp Vibration Control Systems*, 3M Industrial Tape and Specialities Division, St. Paul MN 55144, 1993.

[10] **Nashif**, **A**., **Jones**, **D**. and **Henderson**, **J**., Vibration Damping, John Wiley and Sons, 1985.

[11] **Plunkett**, **R**. and **Lee**, **C**., *Length optimization for constrained viscoelasticlayer damping*, The Journal of the Acoustical Society of America, Vol. 48, No. 1, pp. 150–161, 1970.